EAST EUROPEAN JOURNAL OF PHYSICS. **4.** 267-273 (2025)
DOI:10.26565/2312-4334-2025-4-24 ISSN 2312-4334

PROPAGATION OF AN AZIMUTHALLY POLARIZED TERAHERTZ LASER BEAMS WITH A PHASE SINGULARITY

Andrey V. Degtyarev, Mykola M. Dubinin, Vyacheslav A. Maslov*, Konstantin I. Muntean, Vladislav S. Senyuta
V.N. Karazin Kharkiv National University, 4 Svoboda Sq., Kharkiv 61022, Ukraine
**Corresponding Author email*: v.a.maslov@karazin.ua
Received June 30, 2025; revised October 14, 2025; accepted November 7. 2025

Analytical expressions are derived to describe the nonparaxial diffraction of modes in a dielectric waveguide resonator for a terahertz laser. The study examines the interaction between azimuthally polarized TE_{0m} (m = 1, 2, 3) modes and a spiral phase plate (SPP), accounting for its different topological charges (n). Using numerical modeling, the emerging physical properties of vortex beams are investigated when they propagate in free space. Vector integral Rayleigh-Sommerfeld transforms are used to study the propagation in the Fresnel zone of vortex laser beams excited by TE_{0m} modes of a dielectric waveguide quasi-optical resonator when they are incident on a phase plate. In the studied modes, in the absence of a phase plate, the field exhibits a ring-shaped transverse intensity distribution along the propagation axis. In this case, the number of rings in the cross-section corresponds to the azimuthal number of modes, and the phase distributions for the transverse components of these modes have opposite signs. The use of a SPP with a topological charge n = 1 changes the structure of the beam field, forming an axial maximum in the transverse profile with an increase in the beam diameter at this maximum compared to the case without a phase plate. At the same time the phase structure of the field for transverse components acquires two-lobe symmetry. When using a SPP with a topological charge n = 2 for the TE_{01} mode the restoration of the ring-like field structure is observed and for the TE_{02} and TE_{03} modes the formation of regions of increased intensity is observed. In this case, the phase distributions of the field components for the TE_{01} and TE_{02} modes acquire a three-lobe spiral structure, whereas those for the TE_{03} mode acquire a multi-lobe spiral configuration.
Keywords: *Terahertz laser; Dielectric waveguide resonator; Spiral phase plate; Vortex beams; Azimuthal polarization; Radiation propagation*
PACS: 42.55.Lt; 42.60.Da; 42.25.Bs; 47.32.C–

1. INTRODUCTION

In recent years, in addition to the development of efficient sources and detectors in the terahertz range [1 – 3], the development of terahertz optics is also necessary to ensure the possibility of specific control and manipulation of such radiation by changing its amplitude, phase, polarization, and even orbital angular momentum (OAM) [4 – 6]. Among various terahertz structured beams, vector beams with inhomogeneous phase and polarization states have shown significant practical value in many fields due to their unique light-field distribution characteristics [7 – 9]. The growing interest in terahertz vector vortex beams is due to the helical dislocations of the wavefront that arise in them. Such vortex beams combine the advantages of terahertz waves and OAM. In particular, terahertz waves have a highly coherent, non-ionizing nature and a high penetrating power, while OAM gives the radiation an additional degree of freedom [10 – 13].

The study of the propagation of vortex terahertz laser beams is of great importance for the development of modern science and technology. The unique polarization state and complex spatial structure of terahertz vortex beams provide a richer multiplexing space for information coding and encryption states. Studying the propagation of such beams allows us to better understand their interaction with various materials, particularly nonlinear media, which is crucial for developing new methods of visualization and diagnostics. In addition, these studies contribute to the development of higher-resolution technologies, which are essential for microelectronics and nanotechnology. In free space, vortices can exhibit a stable wavefront structure, allowing them to maintain their unique properties over large distances [14, 15].

Spiral phase plates (SPP), q-plates, achromatic polarization elements, diffraction optical elements, metasurfaces, polarization gratings are used to form vortex beams [9, 16]. SPPs are effective devices for the conversion of various types of beams into vortex beams due to their low fabrication cost, design simplicity and compactness [17, 18].

Optically pumped terahertz molecular lasers are among the first lasers developed in the terahertz range [19]. They have a narrow generation linewidth ($\Delta\nu \approx 1$ kHz) and are among the most powerful tabletop terahertz sources available [20 – 22]. Most optically pumped lasers use waveguide resonators, enabling the generation of sufficiently high powers (up to 1 W) in continuous mode with relatively small cavity sizes [23 – 25]. Among the resonator modes with nonuniform polarization of radiation the TE_{0m} modes with azimuthal polarization have the lowest energy losses and can be effectively used in orbital angular momentum division multiplexing applications in wireless communications [26 – 28].

Cite as: A.V. Degtyarev, M.M. Dubinin, V.A. Maslov, K.I. Muntean, V.S. Senyuta, East Eur. J. Phys. 4, 267 (2025), https://doi.org/10.26565/2312-4334-2025-4-24

The present work is aimed to obtain analytical expressions for describing the nonparaxial diffraction of azimuthally polarized TE_{0m} modes of a dielectric waveguide resonator of a terahertz laser during their interaction with a spiral phase plate, as well as to investigate the spatial structure and evolution of the intensity and phase of the formed vortices.

2. THEORETICAL RELATIONSHIPS

The propagation of laser radiation in free space along the z axis is described by the well-known Rayleigh-Sommerfeld integrals. We use the following expressions of the field components for the cylindrical coordinate system in different diffraction zones [29–31]:

$$E_x(\rho,\beta,z) = -\frac{i\,z}{\lambda r_1^2}\exp(ikr_1)\int_0^{\infty}\int_0^{2\pi} E_x^0(\rho_0,\varphi)\exp\left(ik\frac{\rho_0^2}{2r_1}\right)\exp\left(-ik\frac{\rho\rho_0\cos(\varphi-\beta)}{r_1}\right)\rho_0\,d\rho_0\,d\varphi, \tag{1.1}$$

$$E_y(\rho,\beta,z) = -\frac{i\,z}{\lambda r_1^2}\exp(ikr_1)\int_0^{\infty}\int_0^{2\pi} E_y(\rho_0,\varphi)\exp\left(ik\frac{\rho_0^2}{2r_1}\right)\exp\left(-ik\frac{\rho\rho_0\cos(\varphi-\beta)}{r_1}\right)\rho_0\,d\rho_0\,d\varphi, \tag{1.2}$$

$$\begin{aligned} E_z(\rho,\beta,z) = \frac{i}{\lambda r_1^2}\exp(ikr_1)\int_0^{\infty}\int_0^{2\pi}\left[E_x^0(\rho_0,\varphi)(\rho\cos\beta-\rho_0\cos\varphi)+E_y^0(\rho_0,\varphi)(\rho\sin\beta-\rho_0\sin\varphi)\right]\times \\ \times\exp\left(ik\frac{\rho_0^2}{2r_1}\right)\exp\left(-ik\frac{\rho\rho_0\cos(\varphi-\beta)}{r_1}\right)\rho_0\,d\rho_0\,d\varphi\,, \end{aligned} \tag{1.3}$$

where $k = 2\pi/\lambda$ is the wave number, λ is the wavelength, (ρ_0,φ) are the polar coordinates in the area where the input field is specified, (ρ,β,z) are the cylindrical coordinates in the observation plane, $E_x^0(\rho_0,\varphi)$ and $E_y^0(\rho_0,\varphi)$ are the complex amplitudes x and y components of the input electric field, respectively, $r_1 = \sqrt{\rho^2+z^2}$.

The modes of the studied dielectric resonator coincide with the modes of a hollow circular dielectric waveguide. Therefore, in the initial plane we define radiation in the form of symmetric azimuthally polarized TE_{0m} modes. The expressions for the Cartesian components of electromagnetic fields of these modes in the source plane $z = 0$ have the following form [32]:

$$\text{TE}_{0m}\text{ mode}\quad \begin{cases} E_x^0(\rho_0,\varphi) = -B_{01}J_1\left(U_{0m}\dfrac{\rho_0}{a}\right)\sin(\varphi), \\ E_y^0(\rho_0,\varphi) = B_{01}J_1\left(U_{0m}\dfrac{\rho_0}{a}\right)\cos(\varphi), \end{cases} \tag{2}$$

where a is the radius of the waveguide, J_1 is the Bessel function of the first kind, U_{0m} are the first roots of the equations $J_1(x) = 0$, $B_{0m} = \dfrac{1}{a\sqrt{\pi}J_2(U_{0m})}$ are the normalizing factors for the TE_{0m} modes.

Consider the interaction of these modes with a spiral phase plate (SPP) with an arbitrary topological charge (n) [33]. Let us place the SPP with an aperture of the same radius a at the output of a waveguide (Fig. 1).

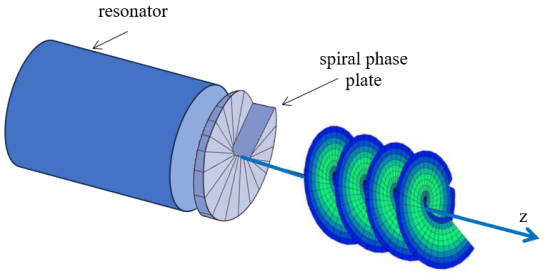

Figure 1. Theoretical scheme of the calculation model of laser beam propagation

The complex transmission function of this SPP in polar coordinates has the form [9]:

$$T_n(\rho_0,\varphi) = \text{circ}\left(\frac{\rho_0}{a}\right)\exp(in\varphi) = \begin{cases} \exp(in\varphi), & \rho_0 \le a, \\ 0, & \rho_0 > a, \end{cases} \tag{3}$$

where circ (·) is the circular function.

To simplify the calculations, integration over the angle φ in (1) can be performed with the known relationships for the integer $\mu > 0$ from [34]

$$\int_0^{2\pi} \cos(\mu\varphi+\varphi_0)\exp[-ix\cos(\varphi-\theta)d\varphi] = 2\pi(-i)^{\mu}J_{\mu}(x)\cos(\mu\theta+\varphi_0)\,,$$

$$\int_0^{2\pi} \sin(\mu\varphi+\varphi_0)\exp[-ix\cos(\varphi-\theta)]d\varphi = 2\pi(-i)^{\mu}J_{\mu}(x)\sin(\mu\theta+\varphi_0)\,.$$

Then from here we can get the following relation

$$\int_0^{2\pi} e^{-ix\cos(\varphi-\beta)}e^{in\varphi}d\varphi = 2\pi\, e^{in\beta}(-i)^n J_n(x)\,. \tag{4}$$

Using Euler's formulas and taking into account Eq. (4), we obtain the expressions:

$$\int_0^{2\pi} e^{-ix\cos(\varphi-\beta)}e^{in\varphi}\sin\varphi\, d\varphi = -\pi e^{in\beta}(-i)^n\ [e^{i\beta}J_{n+1}(x)+e^{-i\beta}J_{n-1}(x)]\,, \tag{5.1}$$

$$\int_0^{2\pi} e^{-ix\cos(\varphi-\beta)}e^{in\varphi}\cos\varphi\, d\varphi = \pi e^{in\beta}(-i)^{n+1}\ [e^{i\beta}J_{n+1}(x)-e^{-i\beta}J_{n-1}(x)]\,. \tag{5.2}$$

Then, using formulas (5.1) and (5.2), we obtain expressions for the field components that describe the nonparaxial diffraction of the TE_{0m} mode on the SPP. They look like this

$$E_x(\rho,\beta,z) = \frac{(-i)^{n+1}k\,z}{2r_1^2}\exp[i(n\beta+kr_1)]B_{0m}\left[\exp(i\beta)G2_{1n+1}(\rho,z)+\exp(-i\beta)G2_{1n-1}(\rho,z)\right], \tag{6.1}$$

$$E_y(\rho,\beta,z) = \frac{(-i)^{n+2}k\,z}{2r_1^2}\exp[i(n\beta+kr_1)]B_{0m}\left[\exp(i\beta)G2_{1n+1}(\rho,z)-\exp(-i\beta)G2_{1n-1}(\rho,z)\right], \tag{6.2}$$

$$E_z(\rho,\beta,z) = \frac{(-i)^{n+1}k\rho}{2r_1^2}\exp[i(n\beta+kr_1)]B_{0m}[G2_{1n+1}(\rho,z)+G2_{1n-1}(\rho,z)], \tag{6.3}$$

where the following notation is introduced

$$G2_{1n\pm1}(\rho,z) = \int_0^a J_1\left(U_{0m}\frac{\rho_0}{a}\right)\exp\left(ik\frac{\rho_0^2}{2r_1}\right)J_{n\pm1}\left(\frac{k\rho\rho_0}{r_1}\right)\rho_0 d\rho_0\,.$$

3. NUMERICAL RESULTS AND DISCUSSIONS

Using expressions (6), the longitudinal and transverse distributions of the total intensity of the electric field ($I=|E_x|^2+|E_y|^2+|E_z|^2$) as well as the transverse distributions of the intensity ($I_i=|E_i|^2$, $i=x,y,z$) and phase $\varphi_i = \mathrm{arctg}(\mathrm{Im}(E_i)/\mathrm{Re}(E_i))$ of individual field components were calculated. The study was performed for laser beams formed by modes of a dielectric waveguide resonator during their interaction with SPP. The calculations were performed for azimuthally polarized TE_{0m} modes (azimuthal number m = 1, 2, 3) at a wavelength of λ = 432.6 μm, which corresponds to the generation line of a THz laser with optical pumping on the HCOOH molecule [35]. The waveguide diameter in the calculations was $2a$ = 35 mm and a phase plate with an identical diameter was installed at its output. In the work the spatial-energy properties of the field of the studied beams were compared for the values of the topological charge of the SPP n = 0, 1, 2.

Fig. 2 shows the longitudinal and transverse distributions of the field intensity of laser beams excited by TE_{01}, TE_{02}, TE_{03} modes in the Fresnel zone in three cases: in the absence of a phase plate (n = 0) and with topological charge 1 and 2. The transverse intensity distributions are plotted in a plane that corresponds to the position of the maximum field intensity along the z-axis. For the studied modes in the absence of a phase plate the field is characterized by a ring transverse intensity distribution along the propagation axis. In this case the number of rings in the cross section corresponds to the azimuthal number of the mode. The introduction of a phase plate with a topological charge n = 1 leads to the formation of an axial maximum in the transverse profile and its displacement toward the radiation source. A further increase in the topological charge to n = 2 returns the beam profile to its initial annular shape, but a decrease in the beam energy localization region is observed.

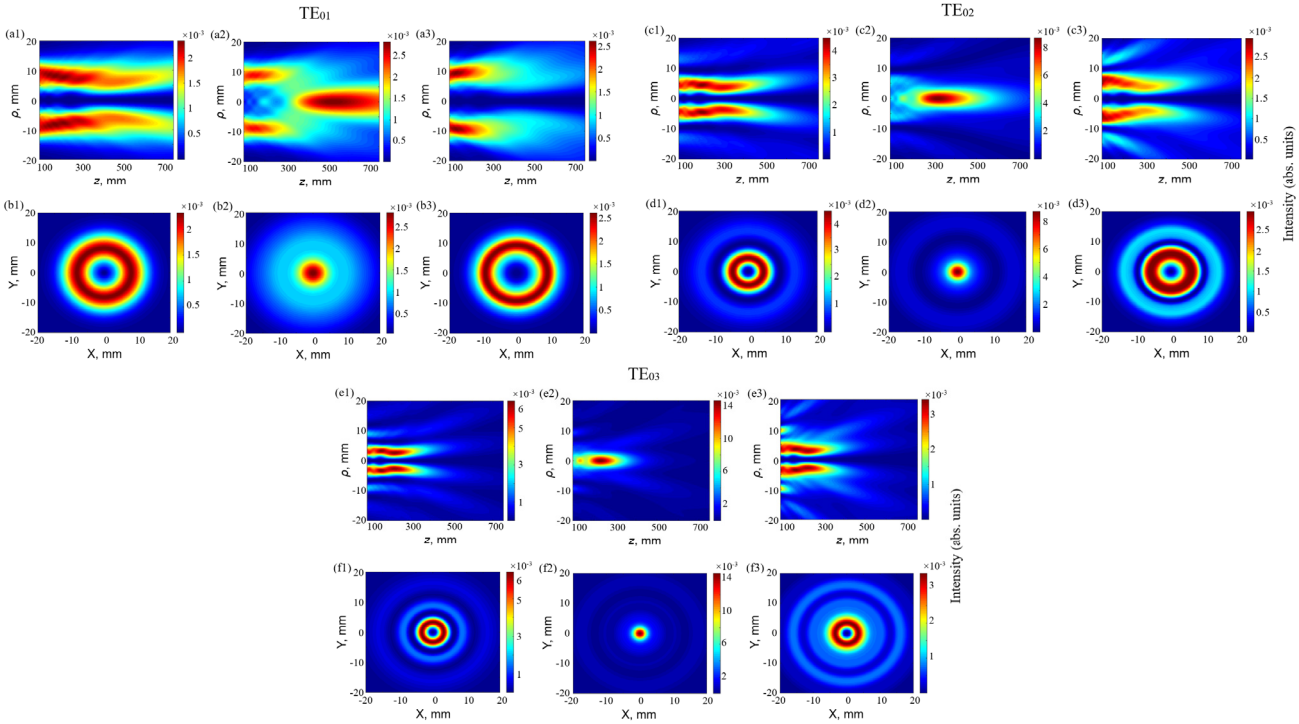

Figure 2. Calculated longitudinal (a1– a3, c1 – c3, e1 – e3) and transverse (b1 – b3, d1 – d3, f1 – f3) distributions of the total field intensity of laser beams excited by TE_{01}, TE_{02}, TE_{03} modes in the Fresnel zone: in the absence of a phase plate (a1, b1, c1, d1, e1, f1), with a topological charge $n = 1$ (a2, b2, c2, d2, e2, f2) and $n = 2$ (a3, b3, c3, d3, e3, f3)

The values of the z coordinates at which the maximum field intensity is achieved and the magnitudes of these intensities as well as the beam diameters are given in Table 1. The diameters of the beams excited by the studied modes were calculated using the formula [36]

$$d = 2\sqrt{\frac{2\int_0^{2\pi}\int_0^{\infty}\rho^2 I(\rho,\beta,z)\,\rho\,d\rho\,d\beta}{\int_0^{2\pi}\int_0^{\infty} I(\rho,\beta,z)\,\rho\,d\rho\,d\beta}}. \qquad (7)$$

Analysis of the obtained results shows that the installation of a spiral phase plate with a topological charge of $n = 1$ compared to the case of its absence is accompanied by a noticeable increase in the beam diameter for all three modes. At $n = 2$ for the TE_{01} mode the beam diameter remains almost unchanged compared to the case without a phase plate, for the TE_{02} mode it decreases, and for the TE_{03} mode on the contrary it increases. The largest value of the beam diameter was obtained for the TE_{03} mode at $n = 1$ and it is $d \approx 40$ mm.

Table 1. Parameters of the studied laser beams excited by TE_{0m} modes in the regions of maximum field intensity at different topological charges.

Mode	n	z (mm)	$I_{max} \times 10^{-3}$ (abs. units)	Beam diameter d (mm)
TE_{01}	0	176	2.33	29.54
	1	527	2.84	38.72
	2	132	2.61	29.87
TE_{02}	0	208	4.48	32.87
	1	321	8.68	39.69
	2	100	2.98	30.42
TE_{03}	0	167	6.44	34.27
	1	231	14.63	40.05
	2	172	3.43	37.79

Figure 3 shows the transverse distributions of the intensity and phase of the Cartesian E_x and E_y components of the electric field for the TE_{01} mode in the Fresnel zone. Since the contribution of the E_z component to the total field intensity is insignificant, its intensity and phase distributions are not presented here or below. In the absence of SPP the field is localized in two areas. However, the phase distributions for the E_x and E_y components exhibit antiphase behavior: the phase changes by π between opposite half-planes according to the orientation of each component. At $n = 1$

characteristic *S*-shaped curvatures appear in the field intensity. The phase distribution for these components in this case takes a spiral shape with two lobes. At $n = 2$ the field is again localized in two regions and the phase distribution acquires a complex three-lobed structure with sharp phase transitions.

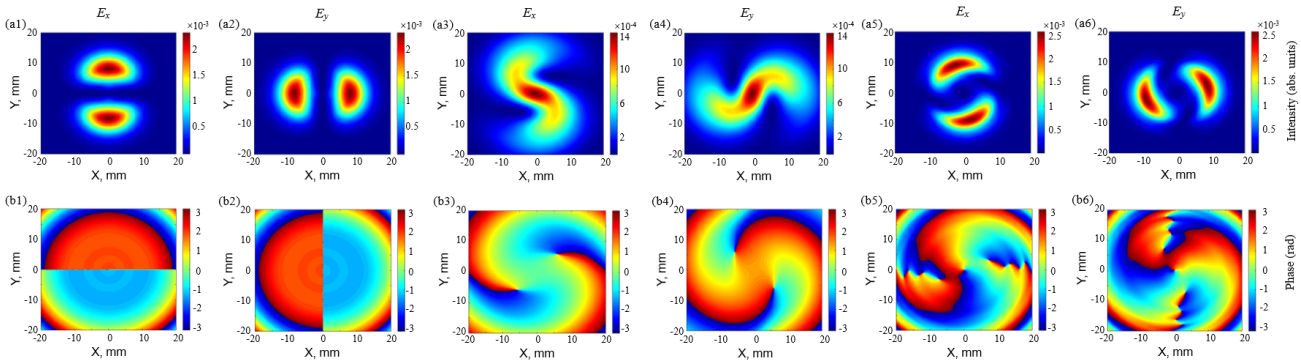

Figure 3. Calculated transverse distributions of intensity (a1 – a6) and phase (b1 – b6) for E_x and E_y components of the field of laser beams excited by the TE_{01} mode in the Fresnel zone: in the absence of a phase plate (a1, a2, b1, b2), with a topological charge of $n = 1$ (a3, a4, b3, b4) and $n = 2$ (a5, a6, b5, b6)

The transverse distribution of the field intensity and phase for the E_x and E_y components of laser beams excited by the TE_{02} mode in the Fresnel zone at different values of the topological charge is shown in Fig. 4. In the case of $n = 0$ the localization of the field energy is observed in four regions. The phase distribution as for the TE_{01} mode exhibits antiphase behavior. At $n = 1$ the maximum field intensity shifts toward the center, and the phase distribution takes on a spiral shape with a characteristic two-lobe structure. At $n = 2$ localization of the field energy in four regions is again observed, but in this case the intensity of the side lobes increases. In this case the phase structure of the field demonstrates clearly defined three-lobe vortices with discontinuities in phase fronts.

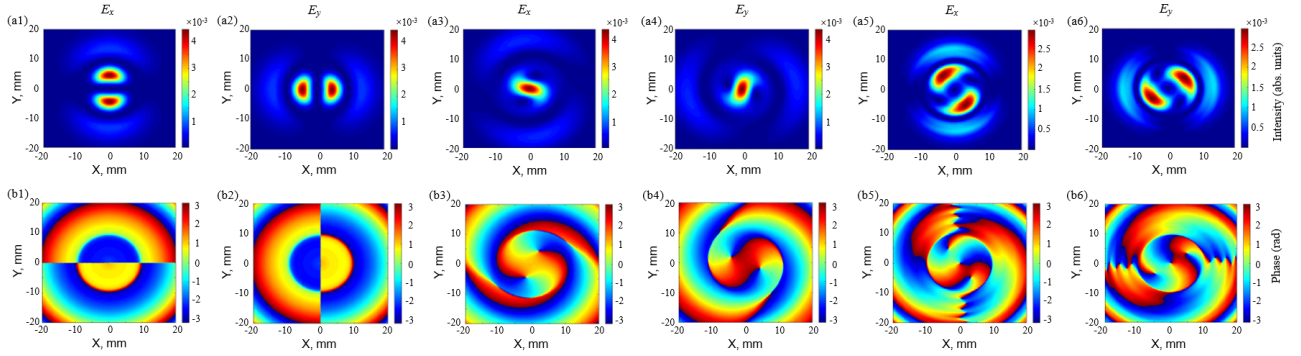

Figure 4. Calculated transverse distributions of intensity (a1 – a6) and phase (b1 – b6) for E_x and E_y components of the field of laser beams excited by the TE_{02} mode in the Fresnel zone: in the absence of a phase plate (a1, a2, b1, b2), with a topological charge of $n = 1$ (a3, a4, b3, b4) and $n = 2$ (a5, a6, b5, b6)

For the TE_{03} mode in the absence of SPP a further increase in the number of field localization regions is observed (Fig. 5). The phase distributions of the studied field components have antiphase symmetry. At $n = 1$ a transformation of the intensity profile appears with energy localization in the central region and the phase distributions acquire a spiral shape. For $n = 2$ a further increase in the energy localization regions is observed with two clearly defined regions of increased field intensity. In this case the phase distributions of the field acquire a multi-lobe spiral structure.

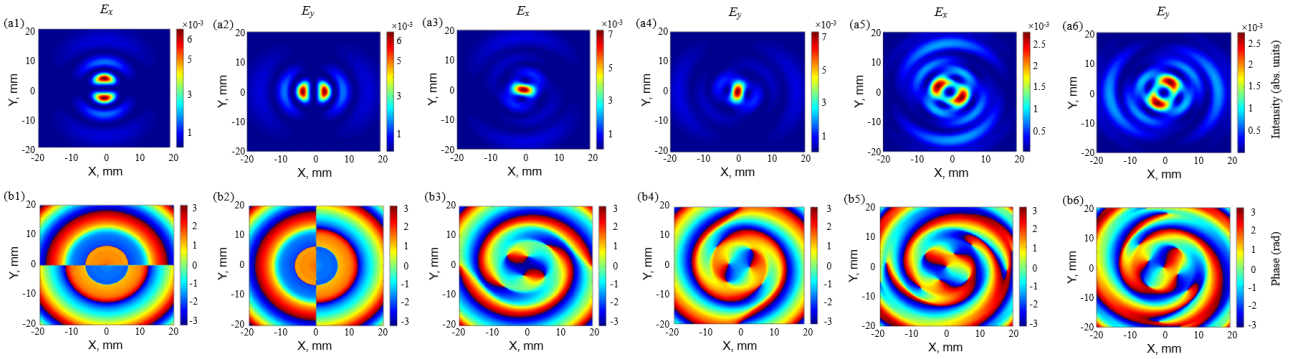

Figure 5. Calculated transverse distributions of intensity (a1 – a6) and phase (b1 – b6) for E_x and E_y components of the field of laser beams excited by the TE_{03} mode in the Fresnel zone: in the absence of a phase plate (a1, a2, b1, b2), with a topological charge of $n = 1$ (a3, a4, b3, b4) and $n = 2$ (a5, a6, b5, b6)

3. CONCLUSIONS

Analytical expressions are obtained to describe the nonparaxial diffraction of TE_{0m} modes (m = 1, 2, 3) of a dielectric waveguide resonator of a terahertz laser during their interaction with a spiral phase plate with its different topological charges (n = 0, 1, 2). The spatial structure of the intensity and phase of the electric field of formed vortex beams during their propagation in the Fresnel zone of free space is investigated.

It is shown that in the absence of a spiral phase plate, when the TE_{01} mode is excited in the resonator, a beam with a ring transverse intensity distribution is formed. The phase distributions for the transverse components of this mode, as well as for the other modes, have the opposite signs. The introduction of a SPP with a topological charge n = 1 leads to the formation of an axial maximum in the transverse profile and an increase in the beam diameter at this maximum compared to the beam diameter in the absence of a plate by almost 10 mm. The phase distribution for a given topological charge takes on a spiral shape with two lobes for all modes. The restoration of the ring-shaped structure is observed at n = 2 with a decrease in the beam energy localization region. In this case, the phase distribution acquires a three-lobe spiral structure.

In the case of the TE_{02} mode without SPP the beam has two pronounced rings in the cross section. At n = 1 a significant increase in the field intensity at the center of the beam is observed and a shift in the localization of radiation energy to its source. For n = 2 the spatial profile of the beam becomes more complex: additional zones of increased intensity appear and the phase exhibits a clear three-lobe structure with discontinuities in the phase fronts. For a given topological charge, the beam diameter has a minimum value.

The TE_{03} mode exhibits the most complex intensity distribution structure already at n = 0 with three rings in the cross section. The introduction of SPP with n = 1 leads to the localization of the field energy in the central region of the beam and a sharp increase in the maximum intensity in this region, which is accompanied by the largest increase in the beam diameter among the studied modes (up to 40 mm). The field structure becomes even more complex at n = 2. Several zones of increased intensity are formed, and the phase distribution acquires a distinct multi-lobe spiral configuration.

ORCID

Andrey V. Degtyarev, https://orcid.org/0000-0003-0844-4282; **Mykola M. Dubinin,** https://orcid.org/0000-0002-7723-9592
Vyacheslav O. Maslov, https://orcid.org/0000-0001-7743-7006; **Konstantin I. Muntean,** https://orcid.org/0000-0001-6479-3511
Vladislav S. Senyuta, https://orcid.org/0000-0001-6601-2379

REFERENCES

[1] J. Freeman, E. Linfield, and A.G. Davies, "Terahertz frequency electronics and photonics: materials and devices," Philosophical Transactions, **383**(2296), 20230378 (2025). https://doi.org/10.1098/rsta.2023.0378
[2] A. Rogalski, "Progress in performance development of room temperature direct terahertz detectors," Journal of Infrared, Millimeter, and Terahertz Waves, **43**(9), 709 (2022). https://doi.org/10.1007/s10762-022-00882-2
[3] A. Leitenstorfer, A.S. Moskalenko, T. Kampfrath, et al., "The 2023 terahertz science and technology roadmap," Journal of Physics D: Applied Physics, **56**(22), 223001 (2023). https://doi.org/10.1088/1361-6463/acbe4c
[4] D. Headland, Y. Monnai, D. Abbott, C. Fumeaux, and W. Withayachumnankul, "Tutorial: Terahertz beamforming, from concepts to realizations, " Apl Photonics, **3**(5), 051101 (2018). https://doi.org/10.1063/1.5011063
[5] A. Siemion, "Terahertz diffractive optics-smart control over radiation," Journal of Infrared, Millimeter, and Terahertz Waves, **40**(5), 477 (2019). https://doi.org/10.1007/s10762-019-00581-5
[6] A. Forbes, "Advances in orbital angular momentum lasers," Journal of Lightwave Technology, **41**(7), 2079 (2022). https://doi.org/10.1109/JLT.2022.3220509
[7] H. Hao, H. Xiaoxue, G. Liping, X. Sixing, and W. Xiaolei, "Research progress of terahertz vector beams," Opto-Electronic Engineering, **51**(8), 240071 (2024). https://doi.org/10.12086/oee.2024.240071
[8] J. He, T. Dong, B. Chi, and Y. Zhang, "Metasurfaces for terahertz wavefront modulation: a review," Journal of Infrared, Millimeter, and Terahertz Waves, **41**(6), 607 (2020). https://doi.org/10.1007/s10762-020-00677-3
[9] H. Wang, Q. Song, Y. Cai, Q. Lin, X. Lu, H. Shangguan, Y. Ai, and S. Xu, "Recent advances in generation of terahertz vortex beams and their applications, " Chin. Phys. B, **29**(9), 097404 (2020). https://doi.org/10.1088/1674-1056/aba2df
[10] J. Lamberg, F. Zarrinkhat, A. Tamminen, M. Baggio, J. Ala-Laurinaho, J. Rius, J. Romeu, E.E. Khaled, and Z. Taylor, "Wavefront-modified vector beams for THz cornea spectroscopy," Optics Express, **31**(24), 40293 (2023). https://doi.org/10.1364/OE.494460
[11] S. Hu, L. Wei, Y. Long, S. Huang, B. Dai, L. Qiu, S. Zhuang, and D. Zhang, "Longitudinal polarization manipulation based on all-dielectric terahertz metasurfaces," Optics Express, **32**(5), 6963 (2024). https://doi.org/10.1364/OE.514410
[12] H. Zhao, X. Wang, S. Liu, and Y. Zhang, "Highly efficient vectorial field manipulation using a transmitted tri-layer metasurface in the terahertz band," Opto-Electronic Advances, **6**(2), 220012 (2023). https://doi.org/10.29026/oea.2023.220012
[13] J. Wätzel, J. Berakdar, and E.Y. Sherman, "Ultrafast entanglement switching and singlet–triplet transitions control via structured terahertz pulses, " New Journal of Physics, **24**(4), 043016 (2022). https://doi.org/10.1088/1367-2630/ac608a
[14] D. Bongiovanni, D. Li, M. Goutsoulas, H. Wu, Y. Hu, D. Song, and Z. Chen, "Free-space realization of tunable pin-like optical vortex beams," Photonics Research, **9**(7), 1204 (2021). https://doi.org/10.1364/PRJ.420872
[15] G. Wang, X. Weng, X. Kang, Z. Li, K. Chen, X. Gao, and S. Zhuang, "Free-space creation of a perfect vortex beam with fractional topological charge," Optics Express, **31**(4), 5757 (2023). https://doi.org/10.1364/OE.483304
[16] X. Wang, Z. Nie, Y. Liang, J. Wang, T. Li, and B. Jia, "Recent advances on optical vortex generation," Nanophotonics, **7**(9), 1533 (2018). https://doi.org/10.1515/nanoph-2018-0072

[17] A.A. Paraipan, D. Gonzalez-Hernandez, I.V. Reddy, G. Balistreri, L. Zanotto, M. Shalaby, R. Morandotti, C. Liberale, and L. Razzari "Scanless spectral imaging of terahertz vortex beams generated by high-resolution 3d-printed spiral phase plates," Small Science, **4**(12), 2400352 (2024). https://doi.org/10.1002/smsc.202400352
[18] K. Miyamoto, K. Suizu, T. Akiba, and T. Omatsu, "Direct observation of the topological charge of a terahertz vortex beam generated by a Tsurupica spiral phase plate," Applied Physics Letters, **104**(26), 261104 (2014). https://doi.org/10.1063/1.4886407
[19] D.T. Hodges, and T.S. Hartwick, "Waveguide laser for the far infrared (FIR) pumped by a CO_2 laser, " Applied Physics Letters, **23**(5), 252 (1973). https://doi.org/10.1063/1.1654878
[20] P. Chevalier, A. Armizhan, F. Wang, M. Piccardo, S.G. Johnson, F. Capasso, and H.O. Everitt, "Widely tunable compact terahertz gas lasers," Science, **366**(6467), 856 (2019). https://doi.org/10.1126/science.aay8683
[21] A. Amirzhan, P. Chevalier, J. Rowlette, H.T. Stinson, M. Pushkarsky, T. Day, H.O. Everitt, and F. Capasso, "A quantum cascade laser-pumped molecular laser tunable over 1 THz," APL Photonics, **7**(1), 016107 (2022). https://doi.org/10.1063/5.0076310
[22] M.-H. Mammez, Z. Buchanan, O. Pirali, et al., "Optically pumped terahertz molecular laser: Gain factor and validation up to 5.5 THz," Adv. Photonics Res., **3**(4), 2100263 (2022). https://doi.org/10.1002/adpr.202100263
[23] R.L. Abrams, and A.N. Chester, "Resonator theory for hollow waveguide lasers," Applied Optics, **13(**9), 2117 (1974). https://doi.org/10.1364/AO.13.002117
[24] G. Li, D. Wang, L. Fang, Z. Ran, and Q. Yan, "Improvement to beam quality of optically pumped terahertz gas lasers with hole-coupling resonators," Optical Engineering, **58**(2), 026104 (2019) https://doi.org/10.1117/1.OE.58.2.026104
[25] O.V. Gurin, A.V. Degtyarev, M.N. Legenkiy, V.A. Maslov, V.A. Svich, V.S. Senyuta, and A.N. Topkov, "Generation of transverse modes with azimuthal polarization in a terahertz band waveguide laser," Telecommunications and radio engineering, **73**(20), 1819 (2014). https://doi.org/10.1615/TelecomRadEng.v73.i20.30
[26] H. Zhou, X. Su, A. Minoofar, et al., "Utilizing multiplexing of structured THz beams carrying orbital-angular-momentum for high-capacity communications," Optics Express, **30**(14), 25418 (2022). https://doi.org/10.1364/OE.459720
[27] H. Wang, and R. Piestun, "Azimuthal multiplexing 3D diffractive optics," Scientific Reports, **10(**1), 6438 (2020). https://doi.org/10.1038/s41598-020-63075-8
[28] H. Ren, X. Li, and M. Gu, "Polarization-multiplexed multifocal arrays by a π-phase-step-modulated azimuthally polarized beam," Optics Letters, **39(**24), 6771 (2014). https://doi.org/10.1364/OL.39.006771
[29] V.V. Kotlyar, and A.A. Kovalev, "Nonparaxial propagation of a Gaussian optical vortex with initial radial polarization," J. Opt. Soc. Am. A, **27**(3), 372 (2010). https://doi.org/10.1364/JOSAA.27.000372
[30] B. Gu, and Y. Cui, "Nonparaxial and paraxial focusing of azimuthal-variant vector beams," Opt. Express, **20**(16), 17684 (2012). https://doi.org/10.1364/OE.20.017684
[31] Y. Zhang, L. Wang, and C. Zheng, "Vector propagation of radially polarized Gaussian beams diffracted by an axicon," J. Opt. Soc. Am. A, **22**(11), 2542 (2005). https://doi.org/10.1364/JOSAA.22.002542
[32] E.A.J. Marcatili, and R.A. Schmeltzer, "Hollow metallic and dielectric waveguides for long distance optical transmission and lasers," Bell Syst. Tech. J., **43(**4), 1783 (1964). https://doi.org/10.1002/j.1538-7305.1964.tb04108.x
[33] J.F. Nye, and M.V. Berry, "Dislocations in wave trains," Proceedings of the Royal Society of London. A. Mathematical and Physical Sciences, **336**(1605), 165 (1974). https://doi.org/10.1098/rspa.1974.0012
[34] B. Gu, and Y. Cui, "Nonparaxial and paraxial focusing of azimuthal-variant vector beams," Opt. Express, **20**(16), 17684 (2012). https://doi.org/10.1364/OE.20.017684
[35] O.V. Gurin, A.V. Degtyarev, N.N. Dubinin, M.N. Legenkiy, V.A. Maslov, K.I. Muntean, V.N. Ryabykh, and V.S. Senyuta, "Formation of beams with nonuniform polarisation of radiation in a cw waveguide terahertz laser," Quantum Electron., **51**(4), 338 (2021). https://doi.org/10.1070/QEL17511
[36] A.V. Degtyarev, M.M. Dubinin, O.V. Gurin, V.O. Maslov, K.I. Muntean, V.M. Ryabykh, V.S. Senyuta, and O.O. Svystunov, "Control over higher-order transverse modes in a waveguide-based quasi-optical resonator," Radio Physics and Radio Astronomy, **27**(2), 49 (2022). https://doi.org/ 10.15407/rpra22.02.49

ПОШИРЕННЯ АЗІМУТАЛЬНО ПОЛЯРИЗОВАНИХ ТЕРАГЕРЦОВИХ ЛАЗЕРНИХ ПУЧКІВ З ФАЗОВОЮ СИНГУЛЯРНІСТЮ

Андрій В. Дегтярьов, Микола М. Дубінін, Вячеслав О. Маслов, Костянтин І. Мунтян, Владислав С. Сенюта
Харківський національний університет імені В.Н. Каразіна, майдан Свободи, 4, Харків, Україна, 61022

Отримано аналітичні вирази для опису непараксіальної дифракції мод діелектричного хвилевідного резонатора терагерцового лазера. Дослідження передбачає взаємодію між азимутально поляризованими TE_{0m} (m = 1, 2, 3) модами та спіральною фазовою пластиною (СФП) з урахуванням її різних топологічних зарядів (n). За допомогою чисельного моделювання досліджено фізичні особливості вихрових пучків, що виникають, коли вони поширюються у вільному просторі. Векторні інтегральні перетворення Релея-Зоммерфельда використовуються для дослідження поширення у зоні Френеля вихрових лазерних пучків, збуджених TE_{0m} модами діелектричного хвилевідного квазіоптичного резонатора, при падінні на спіральну фазову пластину. Для досліджуваних мод за відсутності фазової пластини поле характеризується кільцевим поперечним розподілом інтенсивності на осі поширення. При цьому кількість кілець у поперечному перерізі відповідає азимутальному номеру мод, а розподіли фази для компонент даних мод мають протилежні знаки. Застосування СФП з топологічним зарядом n = 1 змінює структуру поля пучків, формуючи осьовий максимум в поперечному профілі зі збільшенням діаметра пучка у даному максимумі у порівнянні з випадком відсутності фазової пластини. Водночас фазова структура для поперечних компонент набуває двопелюсткової симетрії. При використанні СФП з топологічним зарядом n = 2 для TE_{01} моди спостерігається відновлення кільцеподібної структури поля, а для TE_{02} та TE_{03} мод – формування областей підвищеної інтенсивності. Фазовий розподіл для компонент поля в цьому випадку для TE_{01} і TE_{02} мод набуває трьохпелюсткової спіральної структури, а для TE_{03} моди – багатопелюсткової спіральної конфігурації.

Ключові слова: *терагерцовий лазер; діелектричний хвилевідний резонатор; спіральна фазова пластина; вихрові пучки; поляризація; поширення випромінювання*